Supplemental Information

Critical role for mast-cell Stat5 activity in skin inflammation

Tomoaki Ando, Wenbin Xiao, Peisong Gao, Siavash Namiranian,
Kenji Matsumoto, Yoshiaki Tomimori, Hong Hong, Hirotaka Yamashita,
Miho Kimura, Jun-ichi Kashiwakura, Tissa R. Hata, Kenji Izuhara,
Michael F. Gurish, Axel Roers, Nicholas M. Rafaels, Kathleen C. Barnes,
Colin Jamora, Yuko Kawakami, and Toshiaki Kawakami

Content

Supplemental Figure S1. Eczematous *Plcb3*$^{-/-}$ mice exhibit high serum IgE, increased transepidermal water loss (TEWL) and strong fibrosis, Related to Figure 1. (A) Serum antibody levels in young and old WT and *Plcb3*$^{-/-}$ mice. (B)TEWL was measured on the shaved neck skin and back of young (6-7 weeks old) and old (7-10 months old) mice using Tewameter® TM 300 (CK electronic GmbH, Cologne, Germany). AD-like skin lesions were observed in the neck, but not back, skin of the old *Plcb3*$^{-/-}$ mice. (C) Skin lesions of spontaneously occurring dermatitis in *Plcb3*$^{-/-}$ (KO) and equivalent anatomical sites in WT mice were stained by Masson Trichrome. Blue staining represents deposition of collagen. Bar, 200 μm. Results in *A-C* are representative of 2 experiments using 3-5 mice per group.

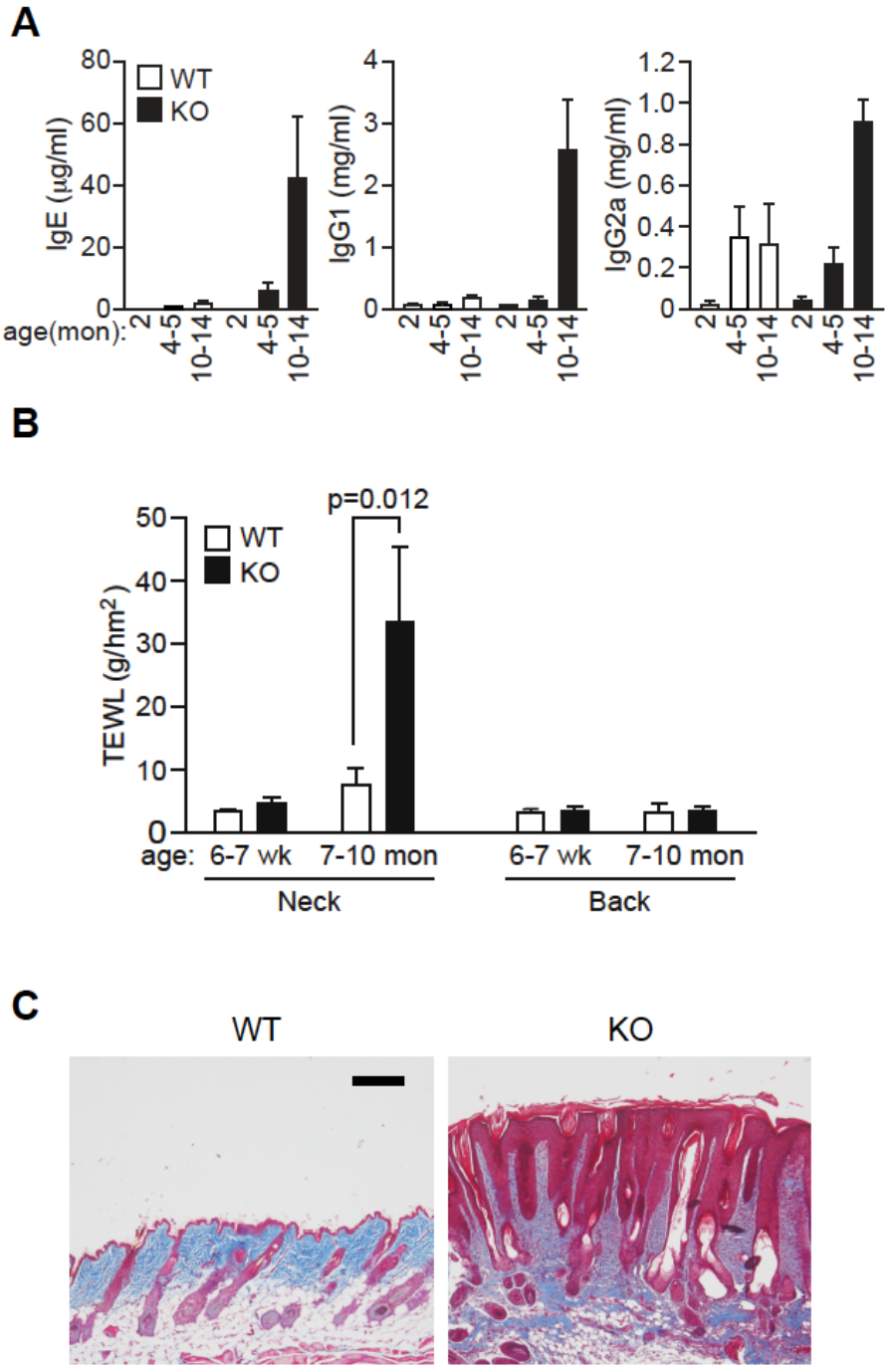

Supplemental Figure S2. Der f/SEB-stimulated *Plcb3*$^{-/-}$ mice have similar levels of serum IgE and IgG1 compared to Der f/SEB-stimulated WT mice, Related to Figure 2. Total serum (A) and Der f-specific (B) immunoglobulins were quantified by ELISA on day 24 (see the Der f/SEB treatment schedule in Figure 2A). (C) AD scores with WT, *FceRIa*$^{-/-}$ (a-), *Plcb3*$^{-/-}$ (b3-), and *FceRIa*$^{-/-}$*;Plcb3*$^{-/-}$ (a-;b3-) mice. Results in *A-C* are representative of 3 experiments using 3-6 mice per group.

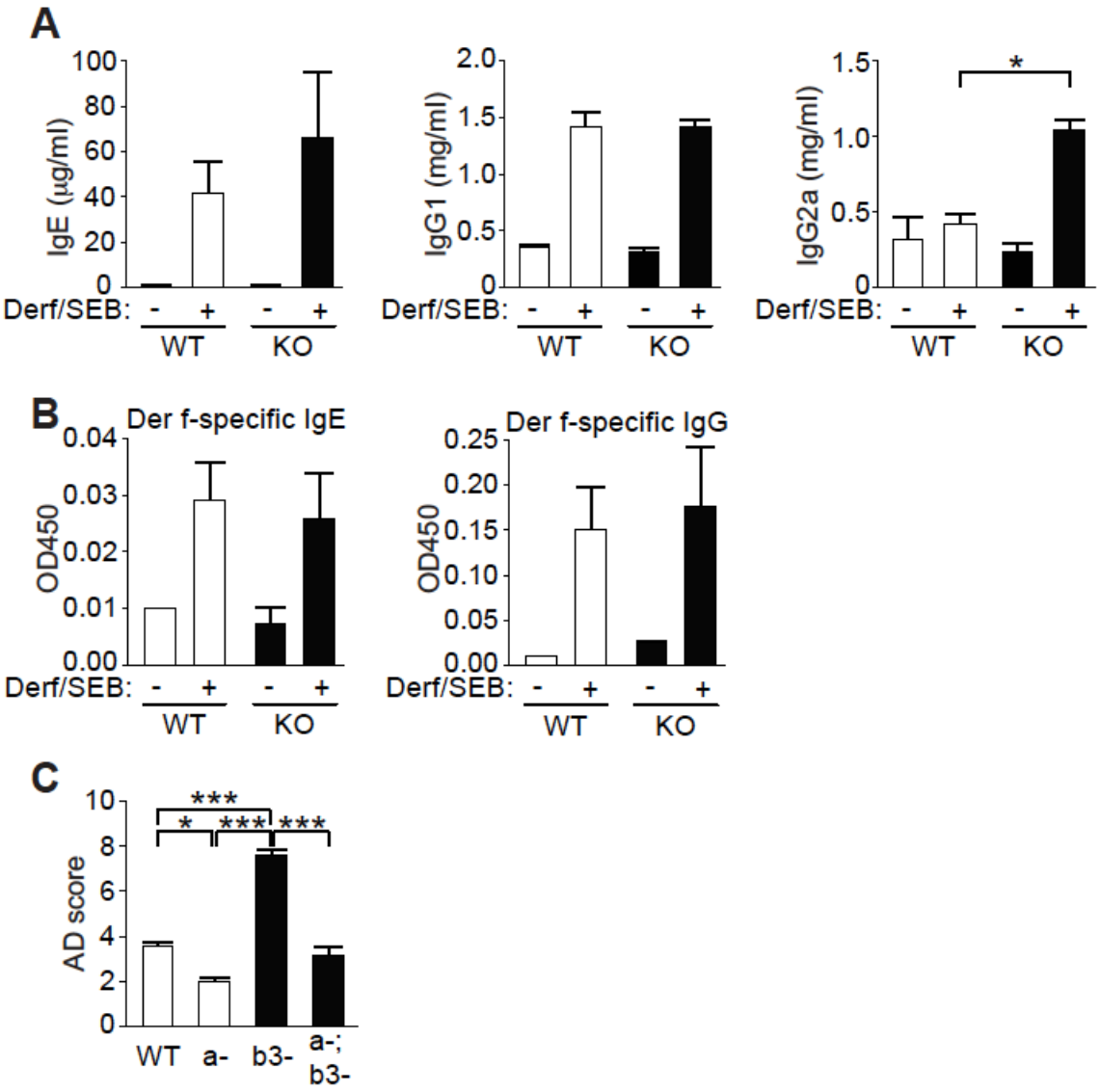

Supplemental Figure S3. *Plcb3*$^{-/-}$ mice have increased BMCPs and MCPs whereas expression of IL-3 and IL-3R was comparable to WT mast cells, Related to Figure 3. (A) Spleen and bone marrow cells from 10 week-old mice were analyzed by flow cytometry. Spleen cells were stained for c-Kit, FcγRII/III, integrin β7, and lineage markers, and c-Kit^{+}Lin^{-} cells were gated for detecting BMCPs. Lin^{-}Sca-1^{-}Ly6c^{-}FcεRI^{-}c-Kit^{+} bone marrow cells were gated for MCPs. *, p<0.05 vs. WT mice by Student's *t*-test. Results are representative of 2 experiments using 3 mice per group. (B) mRNAs for IL-3 or IL-3R components were quantified by microarray for ear skin tissues from 10 week-old WT and *PLC-β3*$^{-/-}$ mice (average of 4 mice each). (C) IL-3R on WT and *PLC-β3*$^{-/-}$ BMMCs was stained for flow cytometry.

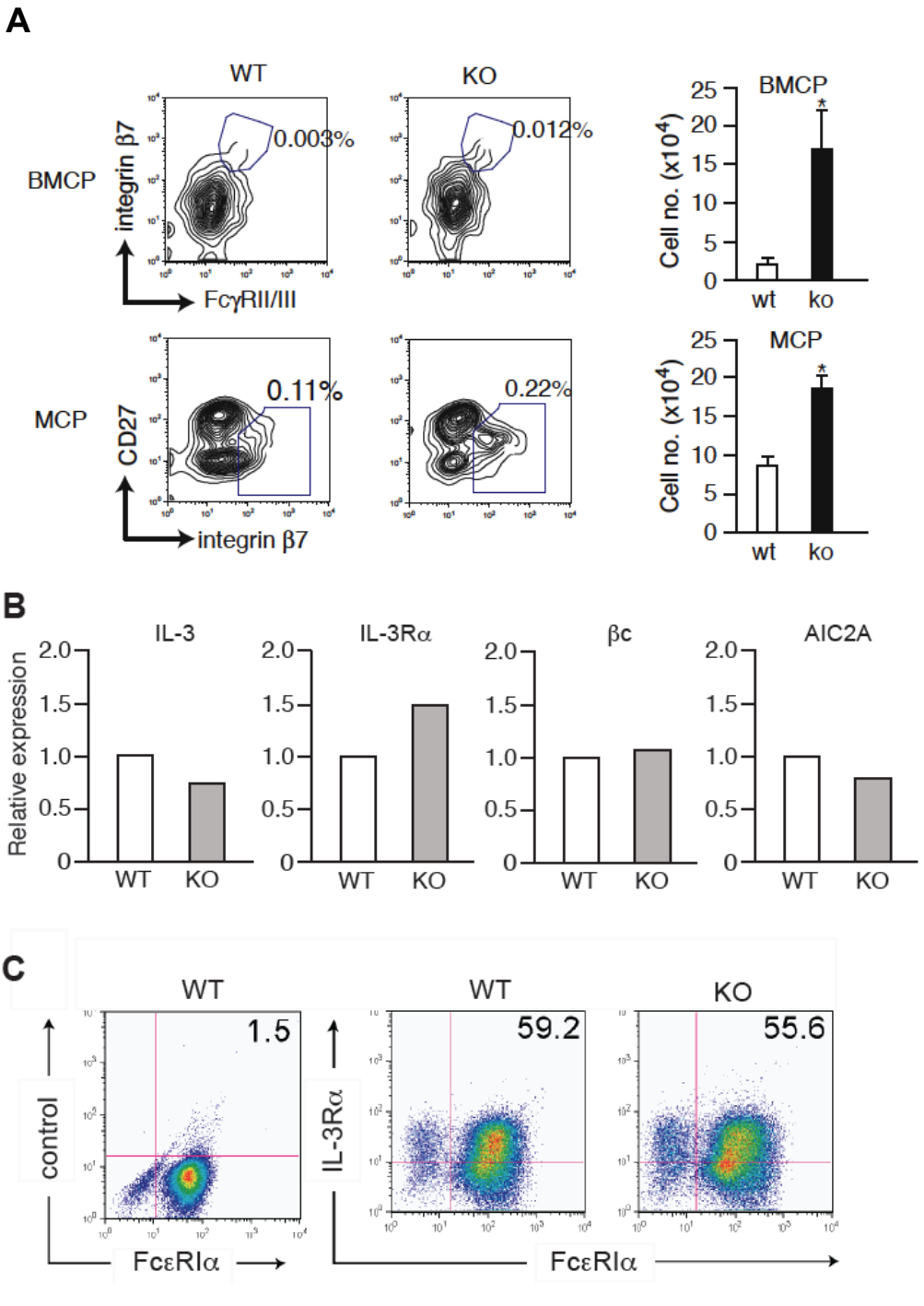

Supplemental Figure S4. Der f/SEB-induced AD scores are increased in *MCΔSHP-1* mice, while JAK Inhibitor TG101348 inhibits Der f/SEB-induced dermatitis, Related to Figure 4. (A-C) Dermatitis was induced with Der f/SEB in *MCΔShp1* mice (CKO or Cre(+)) and their floxed control (fl/fl or Cre(-)) mice. (A) Loss of expression of the targeted loci was confirmed by immunofluorescence microscopy of skin mast cells of MCΔShp1 (CKO) and control (fl/fl) mice. Arrowheads indicate mast cells. (B) Accumulated AD scores from 2 experiments. *, p<0.05 by Student's *t*-test. (C) Mast cells in the ears were stained with toluidine blue. HPF, high-power field. (D-H) B6 mice were co-treated epicutaneously with 100 μM TG101348 along with Der f/SEB. (D) AD scores. (E) Thicknesses of epidermis and dermis after Der f/SEB treatment. Veh, vehicle. (F) Histologic analysis of Der f/SEB-induced dermatitis. Immunofluorescence confocal microscopy was performed to detect TSLP (G) and periostin (H). Results in *D-H* are representative of 2 experiments using 3-5 mice per group.

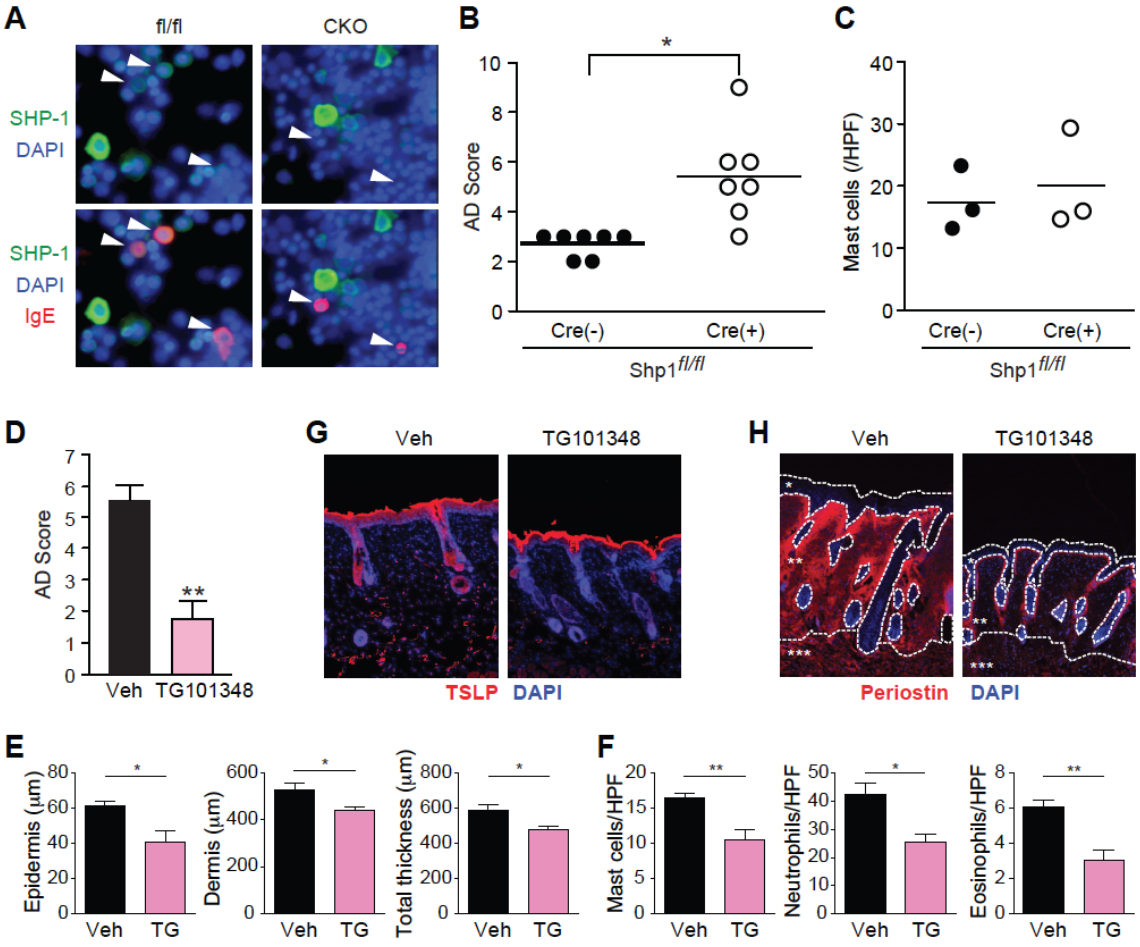

Supplemental Figure S5. TSLP expression in the skin and synergistic mast cell cytokine production by TSLP and FcεRI stimulation, Related to Figure 5. (A) Dermatitis was induced with Der f/SEB in WT, *Kit*$^{W\text{-}sh/W\text{-}sh}$, *Plcb3*$^{-/-}$, and *Plcb3*$^{-/-}$;*Kit*$^{W\text{-}sh/W\text{-}sh}$ mice. Lesional skin was stained for TSLP (red) and nuclei (blue). Borders of epidermis, dermis and subcutaneous fat tissues are indicated by dotted lines. (B) TSLP mRNA was quantified by qPCR with cultured keratinocytes derived from WT and *Plcb3*$^{-/-}$ mice. 18S RNA was used as a control. Results are representative of 2 experiments using 3 mice per group. (C) WT and *TSLPR*$^{-/-}$ (R-) BMMCs were sensitized with anti-DNP IgE and incubated with the indicated concentrations of antigen in the presence or absence of skin extract (Skin Ex) from WT mice. IL-13 and IL-6 secreted into culture media for 20 h were measured by ELISA. Note 1) that skin extract did not contain measurable amounts of IL-13 or IL-6, but skin extract alone induced cytokine production in BMMCs, 2) that antigen stimulation synergized with skin extract to induce cytokine production, and 3) that both IL-13 and IL-6 production induced by skin extract was lower by 20-30% in *TSLPR*$^{-/-}$ BMMCs than in WT BMMCs, except when BMMCs were stimulated with an optimal antigen concentration (10 ng/ml). Therefore, TSLP in skin extract enhances cytokine production by FcεRI-stimulated BMMCs. Essentially identical results were obtained using skin extract from Der f/SEB-treated skin (data not shown). *, $p<0.05$ by Student's *t*-test. Results in *C* are representative of 3 independent experiments.

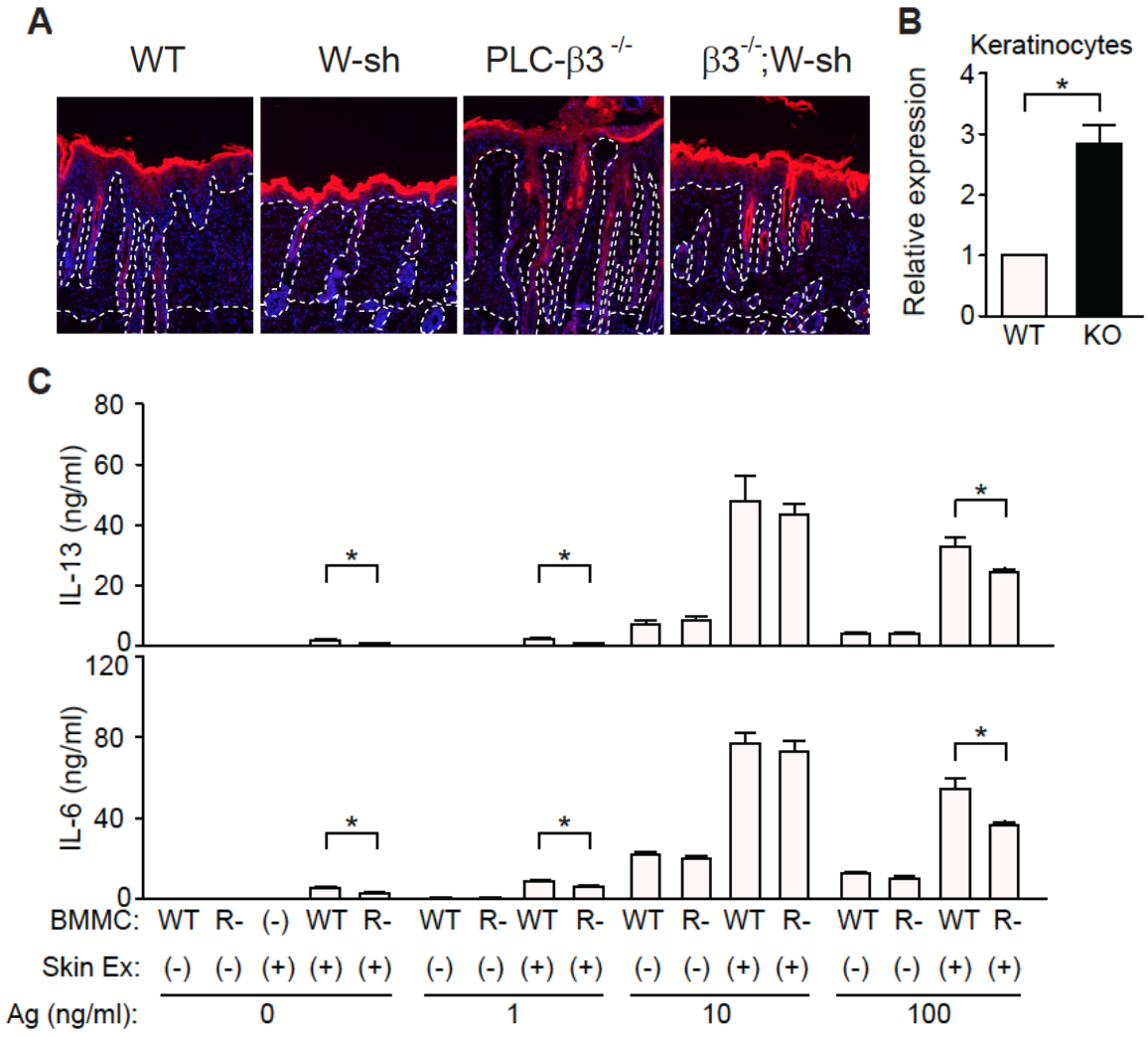

Supplemental Figure S6. Correlation between mast cell numbers and nuclear phospho-STAT5 levels in mast cells among human AD and healthy individuals and inverse correlation of STAT5 phosphorylation with PLC-β3 expression in mast cells in human skin, Related Figure 7. (A) SNP analysis on AD patients (ADEH+ and ADEH-) indicates an association of rs35169799 in *PLCB3* with log-transformed mean serum levels of total IgE (KU/L) in non-atopic European American subjects. (B) Pearson's correlation coefficients were calculated on the data in Figure 7. All data points were calculated (Total) or data points were divided into two groups based on the presence or absence of phospho-STAT5 upregulation in lesional mast cells. The results suggest the presence of two subsets of AD patients with vs. without increased phospho-STAT5 levels in lesional mast cells. **(**C) Skin samples of AD patients were stained for PLC-β3 (red), tryptase (green), and nuclei (blue). Representative images are shown from patient P4. (D-F) PLC-β3 levels in mast cells in lesional (L) and nonlesional (NL) skin samples of AD patients and healthy skin (H) were measured by Image J software (NIH). Skin sample from patient P2 was not available for this analysis due to sample shortage. (D) Data represent mean ± SEM. *, **, ***, ****: p<0.05, 0.01, 0.001, 0.0001 by Student's *t*-test. (E) Median of nuclear pSTAT5 intensity is plotted against that of PLC-β3 intensity. Linear regression curve (solid line) and the 95% confidence interval (dotted lines) are overlaid. Pearson's correlation is shown. (F) Nuclear pSTAT5 intensity in mast cells was compared between lesional and nonlesional skins. Patients are stratified by the presence or absence of a decrease of PLC-β3 expression in panel D. **, p<0.01; ****, p<0.0001 by Tukey's multiple comparison (ANOVA).

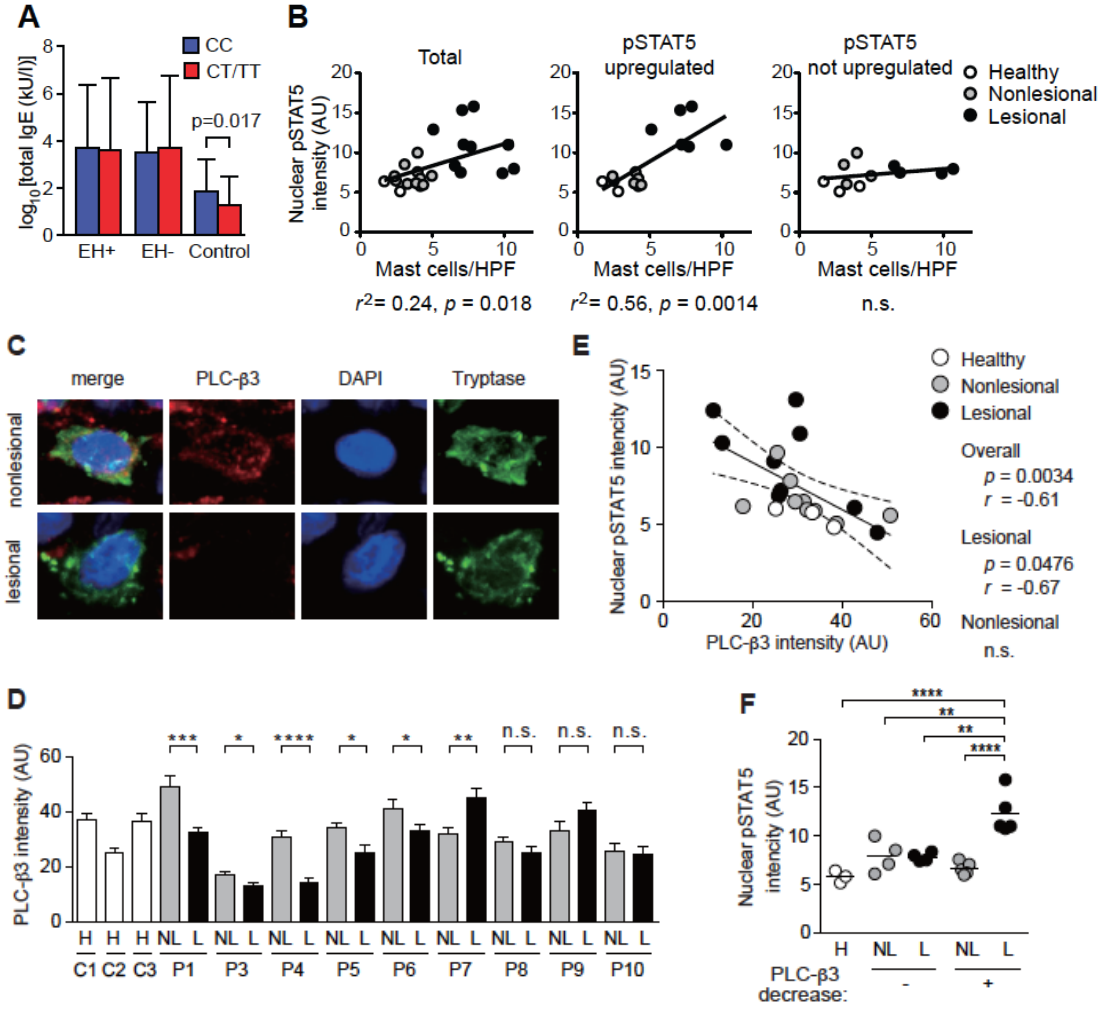

Supplemental Figure S7. Hypothetical vicious cycle of allergic skin inflammation consisting of T_H2 cytokines (secreted from T_H2 cells and mast cells)-periostin (secreted from fibroblasts)-TSLP and other proinflammatory cytokines (secreted from keratinocytes), Related to Figure 6. (A) Allergen-specific T_H2 cells stimulate production/secretion of periostin from fibroblasts. Then, periostin in turn stimulates keratinocytes to produce and secrete TSLP and other inflammatory cytokines. In this scheme, T_H2 cells seem to be required for initial epidermal overexpression of TSLP. Once sustained overexpression of TSLP is established, mast cells may play a more important role in persistent dermatitis than T_H2 cells. PLC-β3 can regulate activities of the cellular elements of this network, such as proliferation of mast cells, periostin production/secretion in fibroblasts and TSLP production/secretion in keratinocytes. Our data also suggest the presence of a feedback loop for inhibition of fibroblasts' periostin production by TSLP and PLC-β3 in fibroblasts is required for this feedback inhibition. DC, dendritic cell; T_H0, naïve $CD4^+$ T cells. (B) Model of SPS complex-mediated mast cell regulation. We showed that SHP-1 efficiently dephosphorylates Stat5 at Tyr^{694} in a PLC-β3-dependent manner in hematopoietic stem cells (Xiao et al., 2009) and mast cells (this study). Our study also showed that Lyn is another member of the SPS complex and that Lyn and SHP-1 regulate each other (Xiao et al., 2010). We propose that SPS members regulate mast cell biology (*e.g.*, proliferation) and AD pathogenesis.

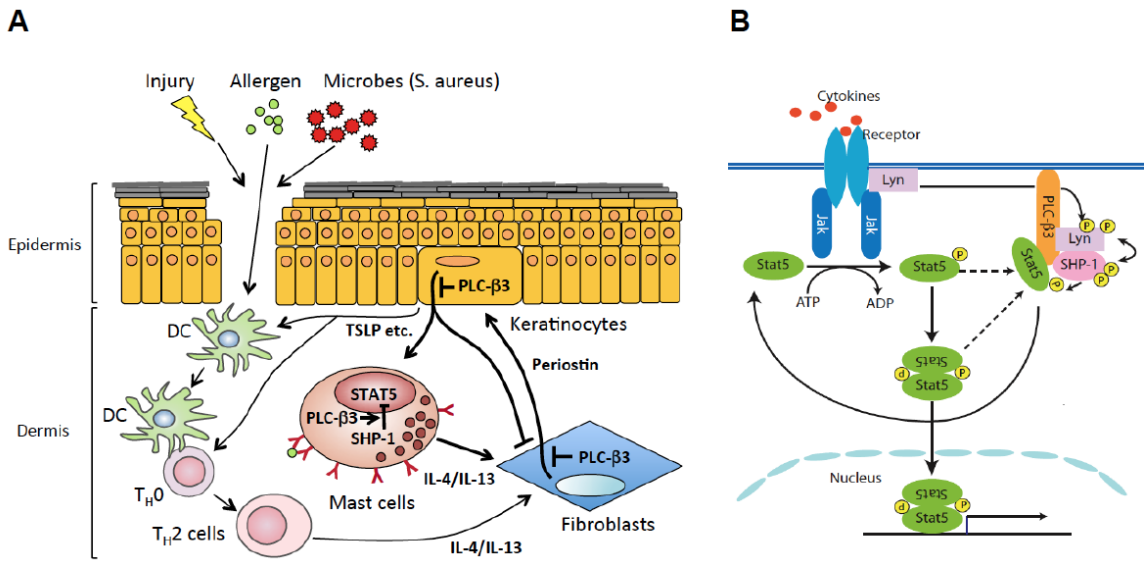

Supplemental Table S1. Similarity of gene expression profiles between spontaneous dermatitis in *Plcb3*$^{-/-}$ mice, Der f/SEB-induced dermatitis in WT mice and human AD, Related to Figure 7.

GEO accession	Orthologs common in the lists	Comparison	*Plcb3*$^{-/-}$ spontaneous skin lesion / WT normal skin		WT Der f/SEB-induced skin lesion / WT normal skin	
			Score	p-value	Score	p-value
GSE6012	10873	AD lesional / Normal skin	1252.7	<0.001	1198.9	<0.001
GSE5667	14325	AD lesional / Normal skin	952.5	<0.001	972.3	<0.001
GSE16161	10873	AD lesional / Normal skin	915.4	0.001	994.1	<0.001
GSE5667	14325	AD lesional / AD non-lesional	961.2	<0.001	1029.0	<0.001
GSE27887	14878	AD lesional / AD non-lesional	941.9	<0.001	1156.9	<0.001
GSE5667	14325	AD non-lesional / Normal skin	350.4	0.556	277.8	0.868
GSE26952	14889	AD non-lesional / Normal epidermis	913.5	<0.001	888.8	<0.001
GSE26952	14889	PS non-lesional / Normal epidermis	600.4	0.003	577.9	0.012

Similarity scores of gene expression changes in spontaneous dermatitis in *Plcb3*$^{-/-}$ mice (vs. normal skin in WT mice), Der f/SEB-induced dermatitis in WT mice (vs. normal skin in WT mice) and human AD (the indicated matches in Comparison column) were computed by OrderedList algorithm. Numbers of the orthologs compared, similarity scores and p-values are shown. For comparison, data with Der f/SEB-induced skin lesions (Ando et al., 2013) and human psoriasis are included.

Supplemental Table S2. SNP identities, location and minor allele frequency in PLCB3, STAT5A, STAT5B and SHP1, Related to Figure 7

Gene (Chromosome)	dbSNP ID	Location	Type of Variant	Risk allele	Allele frequency	
					European American (N=156)	African American (N = 152)
PLCB3	rs2244625	63782720	Coding exon	G	0.328	0.772
(11q13.1)	rs915987	63784464	Intron	A	0.141	0.030
	rs35169799	63787817	Coding exon	T	0.057	0.020
	rs3815362	63790131	Intron (boundary)	T	0.340	0.093
STAT5A	RS16967637	37699948	Intron	A	0.349	0.391
(17q21.2)	RS7217728	37700927	Intron	T	0.652	0.366
	RS13380828	37701981	Intron	A	0.010	0.259
	RS9906989	37709372	Intron	T	0.181	0.173
	RS2272087	37713088	Intron (boundary)	G	0.187	0.254
	RS2293154	37714529	Intron (boundary)	T	0.186	0.171
STAT5B	rs17500235	37609886	Intron	C	0.056	0.010
(17q21.2)	rs9900213	37629407	Intron	A	0.206	0.541
	rs6503691	37647616	Intron	A	0.138	0.612
	rs17591972	37652970	Intron	G	0.103	0.185
SHP1	RS7310161	6927395	Promoter	A	0.560	0.204
(12p13.31)	RS7966756	6932652	Intron	A	0.063	0.454
	rs10744724	6935542	Intron	C	0.059	0.507
	RS759052	6939881	Intron (boundary)	T	0.122	0.431

Supplemental Table S3. Demographic characteristics of AD and control populations, Related to Figure 7

Characteristics	European American		African American	
	AD	Healthy	AD	Healthy
No. of subjects	248	156	171	152
Males; N (%)	91 (36.7%)	63 (40.4%)	40 (23.4%)	77 (50.7%)
Age (yr); mean (SD)	33.1 (18.5)	36.6 (13.2)	35.3 (12.5)	41.1 (10.3)
Geometric mean IgE levels (95%CI)	694.1 (522-922)	59.1 (48-111)	504.8 (378-1229)	141.2 (113-299)
Geometric EASI score (95%CI)[†]	4.6 (3.9-5.4)	NA	3.7 (3.0-4.5)	NA

The following abbreviations used are: AD, atopic dermatitis; EASI, eczema area and severity index; and NA, not applicable. [†]EASI score is determined by the percentage of eczema area on a 7-point ordinal scale: 0 =<10%; 1=10%-29%; 3=30%-49%; 4=50%-69%; 5=70%-89%; and 6=90%-100%.

Supplemental Table S4. Association between SNPs in PLCb3, STAT5A, STAT5B and SHP1 and AD and related phenotypes, Related to Figure 7

Gene and SNP	Position (Mb)	Risk allele	AD				ADEH				EASI	
			European American		African American		European American		African American		African American	
			OR (95%CI)†	P	OR (95%CI)	P	OR (95%CI)	P	OR (95%CI)	P	Beta	P
PLCB3												
rs2244625	63.783	G	1.03 (0.72, 1.48)	0.87	0.98 (0.66, 1.44)	0.904	1.62 (1.06, 2.48)	**0.027***	0.82 (0.33, 2.05)	0.678	0.028 (-0.14, 0.19)	0.738
STAT5A												
rs16967637	37.7	A	0.74 (0.53, 1.04)	0.08	0.91 (0.63, 1.31)	0.609	0.83 (0.54, 1.29)	0.411	1.31 (0.63, 2.74)	0.466	0.151 (0.00, 0.30)	**0.048**
STAT5B												
rs9900213	37.629	A	0.66 (0.44, 99)	**0.045**	0.87 (0.61, 1.24)	0.448	1.4 (0.86, 2.30)	0.18	1.74 (0.76, 3.99)	0.191	0.075 (-0.07, 0.22)	0.32
SHP1												
rs7310161	6.927	T	1.55 (1.10, 2.17)	**0.012**	1.32 (0.86, 2.03)	0.207	1.05 (0.72, 1.54)	0.694	0.85 (0.34, 2.13)	0.735	-0.226 (-0.40, -0.05)	**0.012**
rs7966756	6.933	A	0.9 (0.47, 1.73)	0.756	1 (0.71, 1.41)	0.99	0.9 (0.38, 2.11)	0.802	1.04 (0.52, 2.08)	0.922	-0.227 (-0.36, -0.10)	**0.0009**
rs10744724	6.935	C	0.95 (0.49, 1.83)	0.875	1.26 (0.90, 1.78)	0.183	0.76 (0.31, 1.87)	0.553	0.72 (0.34, 1.50)	0.376	-0.258 (-0.39, -0.12)	**0.0003**
rs759052	6.94	T	1.07 (0.66, 1.75)	0.785	1.3 (0.92, 1.84)	0.139	0.69 (0.36, 1.34)	0.272	0.42 (0.22, 1.14)	0.101	-0.241 (-0.38, -0.10)	**0.001**

*P=0.006 when analysis was done in a recessive model.
†Allelic odds ratios